Three-Dimensional Single Step Flow Sheathing in Micro Cell Sorters

G. Goranovic[1], I.R.Perch-Nielsen[2], U.D.Larsen[3], A.Wolff[2], J.P.Kutter[1], P.Telleman[4]

[1]μTAS project, Mikroelektronik Centret, Oersteds Plads, 2800 Lyngby, Denmark, gg@mic.dtu.dk
[2]Cell Sorting project, Mikroelektronik Centret, Lyngby, Denmark, irp@mic.dtu.dk
[3]Chempaq, Lyngby, Denmark,
[4]Mikroelektronik Centret, Lyngby, Denmark

ABSTRACT

We present a novel microstructure that enables 3 dimensional hydrodynamic focusing of cells in a pressure driven micro cell sorter. This so-called "chimney" structure for single step coaxial sheathing was designed and optimized through simulation, and then successfully micromachined in silicon as part of an integrated micro cell sorter. Coaxial sheathing was clearly demonstrated by velocity distribution experiments and shown to be in accordance with simulation data. The "chimney" structure is easy to machine and can be monolithically integrated with a variety of other microfluidic structures.

Keywords: Cell sorting, microfluidics, coaxial sheathing, simulations

INTRODUCTION

Cell sorting plays an important role in research and medical diagnostics. The realization of cell sorting in microstructures provides many advantages over conventional fluorescent activated cell sorting (FACS), including low consumption of sample and sheathing buffer, closed systems that reduce risk of infection of the sorted cells and reduce potential biohazard risks, feasibility of making portable instruments and single use devices [1]. The most important feature is however that microsystems allow functional integration thereby providing overall improved performance, e.g. sample preparation and DNA amplification. Cell sorting in microstructures is based on laminating cells with buffer and selecting cells of interest by flow switching (Figure 1). In the first generation micro cell sorters, sample was sheathed (focused) sidewise but not on top or bottom. Characteristic for laminar flow [2], cells in different vertical positions in the channel travel at different speeds. These differences in speed made it difficult to accurately adjust time switching for sorting cells of interest. To eliminate these difficulties, the second generation cell sorter was devised to enable hydrodynamic focusing from all sides. This three dimensional sheathing should provide more uniform velocity distribution in the core sample stream [3] allowing better timing of flow switching and thereby improve sorting efficiency (Figure 2).

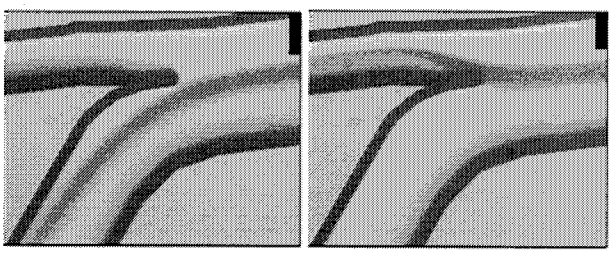

Figure 1: Flow switching in a micro cell sorter

SIMULATIONS

Simulations are an indispensable tool in the development process of microsystems giving us better insight in the nature and functioning of microscale phenomena. Also, optimizing the structures before the fabrication process substantially reduces costs and turn-around times.

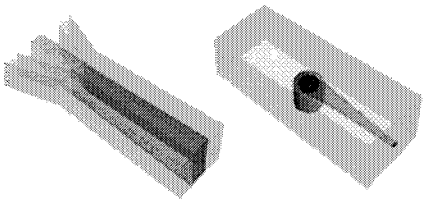

Figure 2: Schematic comparison between 2D and 3D sheathing

In this study simulations were performed with the CFD-ACE+ 6.2 software (CFD Research Corporation, Huntsville Alabama), a multiphysics package based on the Finite-Volume Method. The program was run on a 800 MHz Pentium III processor with 256MB of RAM memory. The mesh-independence test runs were made within the range between 15000 and 48000 cells. Although operated in the laminar flow regime, a rather fine mesh was needed to account for the more complex geometry of the design that was fabricated and experimentally examined. The time for each calculation spanned from 20 minutes up to 2 hours.

As reported by Gravesen et al [4], the definition of the transitional Reynolds number between the viscous and the inertial regimes in microfluidics needs to be altered since most of the times the characteristic lengths in the direction

of flow are shorter than the entrance lengths for fully developed flow. In that sense the transitional Reynolds number in microfluidics can be described as:

$$Re_t = \frac{C}{\xi}\frac{L}{D_h} \quad (1)$$

where C is the friction coefficient (C=64 for circular cross section, C=96 for rectangular cross section with w>>h), ξ=41 for a slit-type orifice, L is length in the direction of flow, D_h is hydraulic radius. In the case of Re > Re_t, the pressure drop is dominated by inertial losses. It can be seen from Table 1 that in microfluidics the transitional Reynolds number can be well below the familiar value of Re=2300.

	L [μm]	D_h [μm]	Flow rate [ml/min]	Re (UD_h/v)	Re_t
chimney (sample)	700	500	0.02	3.3	2.2
		100	0.02	0.7	10.9
channel (sheath)	1000	167	0.01	0.6	14
			0.05	2.8	14
			0.1	5.6	14
			0.3	16.7	14
			0.5	27.8	14

Table 1: Geometry and flow parameters of the structures on which the measurements were performed

The idea for the chimney structure was inspired by simulations, before it was actually fabricated [3]. In order to examine the impact of different geometries, additional simulations were performed simulating the actual fabricated design in several regimes of Reynolds numbers (see Table 1). The dimensions of the structures were taken from the actual masks used in the fabrication process (tube inner diameter: 500 μm, 100 μm; channel width: 500 μm, channel height: 100 μm). In Figure 5 top and side views are shown of the sample concentration distributions in the device for values of the sheath-to-sample-flow-rate ratio σ equal to 0.5, 5 and 25, respectively. In Figure 3, the performance of the chimney structure with a 100 μm diameter is shown, together with the vertical velocity distribution and a concentration isosurface.

According to the simulations, there are several trends to be observed:

- sheathing of the core sample stream increases when σ increases
- sheathing of the core sample stream decreases when inner diameter of the chimney's sample inlet increases (due to a higher sample volume per unit time)
- the vertical velocity distribution within the sample in the outlet channel is more uniform as compared to the overall vertical velocity distribution in that part of the channel (due to confinement to a smaller region).

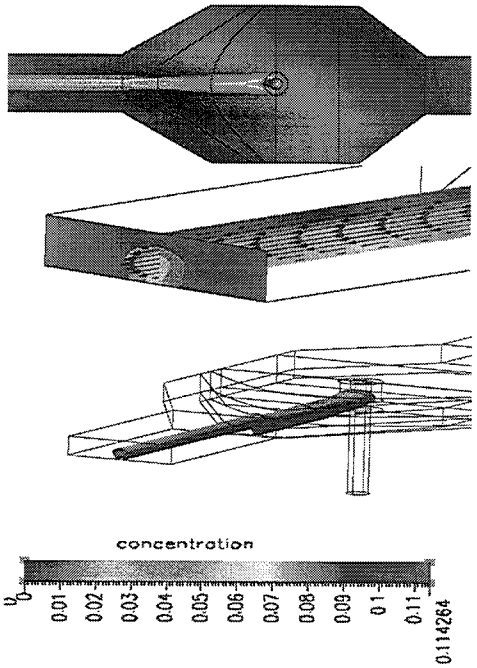

Figure 3: Sheathing with 100 μm chimney. Velocity distribution in the sample stream and 80% concentration isosurface are shown.

FABRICATION

The device was fabricated in silicon in a three-step process of reactive ion etching (RIE) in a plasma of SF_6 and O_2. In the first step, the front etching of the 50 μm deep basin (lowest part of the chimney) and the inner part of the circular tube was made using the first mask. In the second step, the 100 μm deep channels were completed (second mask). Finally, the hole for the sample inlet was made in the 250 μm deep etching from the backside of the wafer (third mask). To complete the structure, a glass lid was anodically bonded on top of the etched geometry. Figure 4 shows a top view of the structure. The inclined walls (seen as thick borders) are a consequence of the underetching that was compensated in later designs by slight modification of the masks.

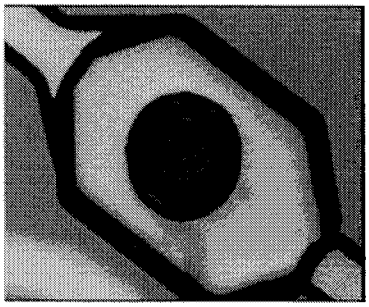

Figure 4: A fabricated chimney structure

EXPERIMENTS

There are substantial challenges concerning the measurements of flow parameters (e.g. the velocity distribution) in microstructures due to a restricted access to the structures. Only recently some of the techniques such as micro PIV (Particle Image Velocimetry) [5] have been successfully adopted to microstructures.

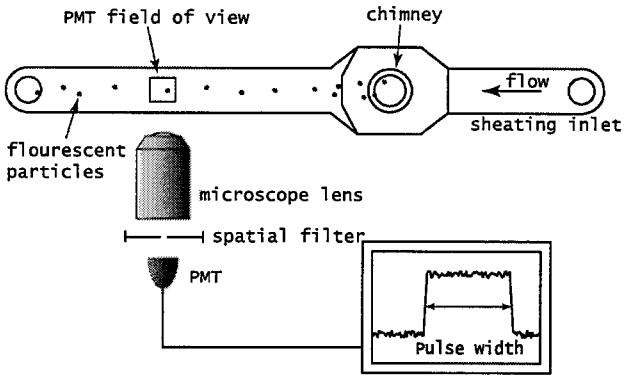

Figure 5: Schematic view of the experimental set-up

Our experiments were performed on the set-up shown schematically in Figure 5. An epi-fluorescent microscope and lenses (Leica Germany) were used with magnifications ranging from 5x (NA=0.12) to 40x (NA=0.55). Sample solutions were a suspension of fluorescent beads (11.95 μm in diameter, λex=458 nm, λem=540 nm, Bangs Labs Inc), and a 0.1% (w/v) phenol red solution. In order to determine the flow speeds, the fluorescent beads in a sample were exited and traced by collecting their emission light with the microscope fitted with a photo multiplier tube, with final processing in an oscilloscope. The light interrogation area was a rectangular spot (L=125 μm, wider than the core stream) positioned downstream in the outlet channel. Obviously, particles with a lower velocity spend more time in the slit, allowing more emission light to be collected. The width of the collected signal is inversely proportional to the velocity.

In a first experiment, the comparison between a 2D-sheathing chip and the 3D-sheathing chimney structure was carried out in order to observe the difference in performance. Dimensions of the outlet channels were the same in both cases (width=500 μm , depth=100 μm). The sheathing liquid was water and the sample solution had a bead density of 4.0×10^5 particles/ml. The results of the velocity distribution are shown in figure 6. It can be clearly seen that the chimney yields a more uniform velocity distribution within the sample stream. This experiment, however, cannot be directly compared against simulations since it does not resolve the velocity contributions coming from beads at different heights of channel.

A second experiment was performed to get more information about the size of the sample stream. This time, fluorescent beads were added to the sheathing liquid while the sample was pure water. The interrogation area was extended to cover the entire width of the channel. Figure 7 shows the total collected light intensity from the beads (normalized over the entire channel depth) as a function of the channel width for various values of sheath-to-sample-flow-rate ratio σ. The size of the sample stream (width and height of the intensity valley) can now easily be observed from the graphs. The measurements confirm the trend seen in the simulations where the sample sheath narrows for higher σ ratios.

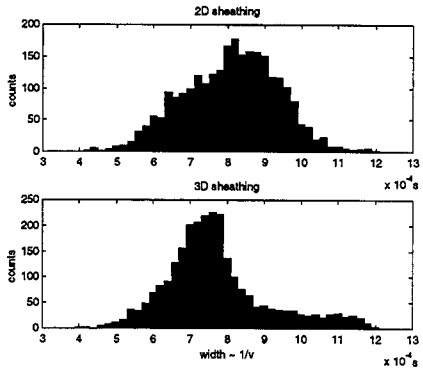

Figure 6: Width distribution of fluorescent signals (~1/velocity) for the 2D and the 3D sheathing. Smaller velocity dispersion is observed in the chimney structure.

Finally, a phenol red solution was pumped through the chimney structure and the sheathing effect was monitored. As seen from figure 8 the agreement with the simulation data is very good. The small discrepancies arise from the fact that diffusivity constant for phenol red was an estimate rather than a known value (estimated to be 10^{-9} m^2/s). Furthermore, differences in geometries of the fabricated structures due to underetching were not taken into account.

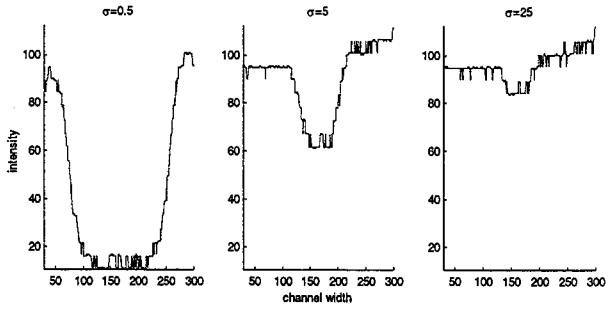

Figure 7: Intensity valley for different σ values. The stream is confined to the middle of the channel. The depth of the coaxial sample stream in the channel could not be determined. Better focusing is obtained for higher σ.

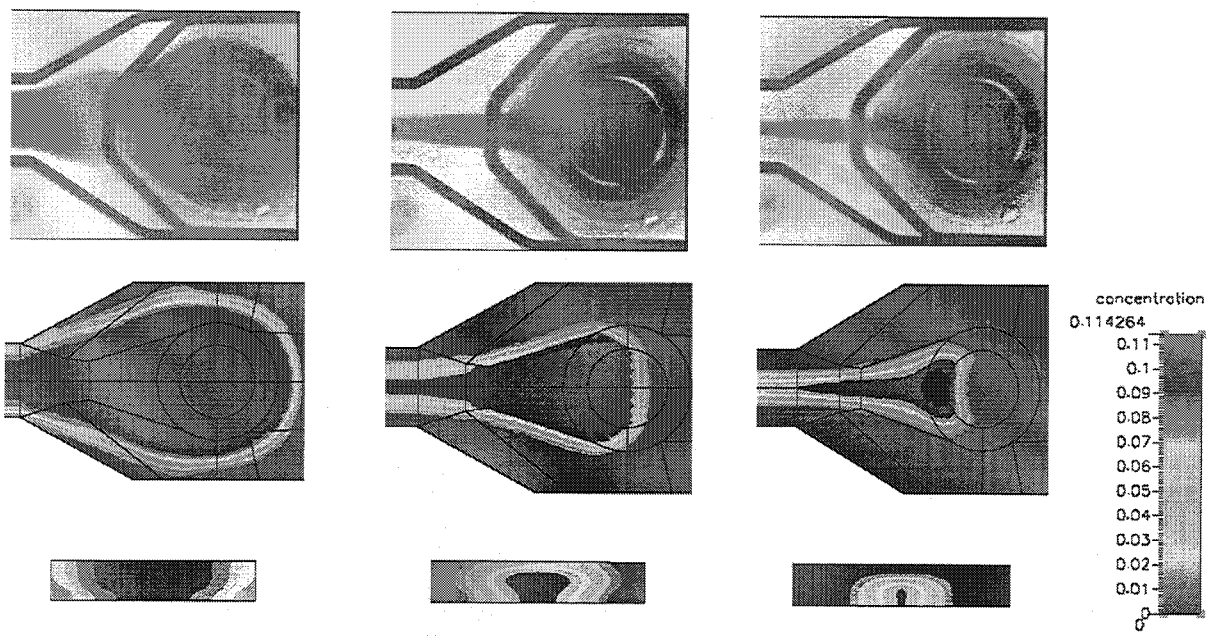

Figure 8: Experimental and simulated flows of phenol red solution for $\sigma = 0.5$, 5 and 25, respectively. Diameter of the chimney is 500 μm . The 3 pictures at the bottom show the cross section of the sample stream in the outlet channel. Dark colors in the middle of the stream represent more than 90% of the concentration. Limited accuracy is due to the approximate value for the diffusivity and slightly different geometry due to underetching.

RESULTS AND DISCUSSIONS

The simulations of the chimney structure have predicted the focusing effect which was then experimentally confirmed. Generally, higher sheathing velocity and smaller chimney diameter produce stronger effects with higher uniform velocity distributions within the sample stream. The simulations and experiments clearly demonstrate the advantages of the 3D over the 2D sheathing principle. However, the actual sample distribution along the depth of the channel could not be obtained due to the limitations of the experimental set-up.

In order to achieve even better agreement between the simulations and the experiments, some refinements are necessary both in the simulation as well as in the experimental part. First, the physical parameters, such as coefficients of diffusion, need to be properly determined. The effects of underetching have to be taken into account to determine whether these small geometrical changes affect performance. Finally, more accurate velocity profiles of particles at the sample inlet need to be determined (with methods like PIV) if the movement of fluorescent beads is to be taken into account.

An experimental set-up for PIV has been constructed which will be employed to further improve determination of the correlation between our models and experimental data. The experiences described in this paper will be used to include simulation as an intrinsic design tool for microstructures with applications in chemistry and life sciences.

ACKNOWLEDGEMENT

The results described in this paper are made in collaboration between the μTAS and the Cell sorting projects at the Mikroelektronik Centret in Lyngby, Denmark. The authors would like to thank to company Chempaq for the valuable input on some of the important issues.

REFERENCES

[1] P. Telleman, et al., Micro tools for cell handling, SPIE conference on microfluidic devices and systems, Sep. 2000, Santa Clara, USA,

[2] A. Wolff, et al., Chip-integrated microfluidic system for cell sorting and cell culturing, Eurosensors 2000, Aug 2000, Copenhagen, DK

[3] U. D. Larsen, et al., Method for providing a coaxial flow in a flowsystem, Patent number DK PA 2000 00409, 2000

[4] P. Gravesen, et al., Microfluidics – a review, J. Micromech. Microeng. 3 (1993), p. 168-182

[5] C.D. Meinhart, et al., PIV measurements of a microchannel flow, Experiments in Fluids 27 (1999), p. 414-419